Soils and Rocks
An International Journal of Geotechnical and Geoenvironmental Engineering
www.soilsandrocks.com
ISSN 1980-9743
ISSN-e 2675-5475

Degradation of a woven polypropylene geotextile in a coastal environment

Rayanne Karlla Santos da Silva[1#], Lucas Araújo dos Santos[2],
Fagner Alexandre Nunes de França[3], Matheus Cardoso dos Santos[4],
Fernando Henrique Martins Portelinha[4]

Article

Keywords
Geosynthetic
Ultraviolet
Durability
Coast protection
Tensile strength
Polypropylene

Abstract

Geobags have been applied in many coastal protection solutions giving them effective performance against cyclic hydrodynamic loading. However, polymer materials, such as the geotextiles used for geobags production, are susceptible to environmental degradation which is critical for engineering applications. This study aims to investigate the durability of woven polypropylene geotextiles under coastal environmental conditions, considering different exposure surface characteristics, such as varied slope surfaces, type of application surface, and surface color. Exposure panels were constructed, and geotextiles samples were exposed to the coast environment of Natal (Brazil) for period reached 492 days, during which specimens were collected, and geotextile tensile properties have been obtained as a reference of material degradation. Results indicated a strength depletion of 35% by the end of the exposure period. No significant influence of surface inclination on degradation was observed, while surface color emerged as a potentially influential factor. The findings of this study are essential for informing the design and implementation of mitigation strategies in coastal engineering works involving geosynthetics.

1. Introduction

Reduction in strength capacity and subsequent failure of geosynthetic materials occur when significant changes are observed in the polymers at the molecular level, in the chemical properties, or even changes in the physical and mechanical properties, under sustained deleterious exposure conditions. All of this is caused by sources that induce the action of degradation agents in the polymers, as discussed by Koerner et al. (1992). Among these sources, high temperatures, oxidation, natural weathering, ultraviolet radiation, and chemical elements can be highlighted (Paula & Pinho-Lopes, 2021). Notably, in specific applications such as coastal protection systems, geosynthetics may be in direct contact with one or more of these degradation agents in real-field environments.

In such applications, geotextile bags are typically filled with sand functioning similarly to rock armoring used in breakwaters, groynes, or dikes. Elias et al. (2022) describes advantages of using geobag technique regarding the geotextile's filtration capacity, allowing them to retain the fill material while dewatering. The authors also report that economic and construction benefits fill materials are locally available compared to the costs involving in acquiring and transporting traditional rockfill elements. As regards geobags for cost protection, Rajabian et al. (2012) describe the proper performance of this solution as subjected to cyclic hydrodynamic loads and the capability of absorbing seabed morphology changes given its flexibility. However, Li et al. (2023) emphasize that the long-term behavior of these structures is dependent on the durability of the geotextile in coast environment. Polymers may suffer rapid degradation with sunlight exposition, mainly when associated with other environmental effects such as temperature and humidity, chemical characteristics of contact and specific characteristics of the region (Hsieh et al., 2006).

Extensive research has been conducted to improve the understanding of the actual impact of geotextile deterioration. Guimarães et al. (2017), for instance, investigated a woven polypropylene geotextile (273 g/m^2) with an initial tensile strength of 56.7 kN/m, subjected to a field exposure test in the city of Varginha, Minas Gerais (Southeastern Brazil; 21.5490°

[#]Corresponding author. E-mail address: rayannekarlla01@gmail.com.
[1]Universidade Federal do Rio Grande do Norte, Departamento de Engenharia Civil, Natal, RN, Brasil.
[2]Universidade Federal do Rio Grande do Norte, Departamento de Engenharia de Produção, Natal, RN, Brasil.
[3]Universidade Federal do Rio Grande do Norte, Departamento de Engenharia Civil e Ambiental, Natal, RN, Brasil.
[4]Universidade Federal de São Carlos, Departamento de Engenharia Civil, São Carlos, SP, Brasil.

Submitted on July 31, 2025; Final Acceptance on October 28, 2025; Discussion open until August 31, 2026.
Editor: Renato P. Cunha
https://doi.org/10.28927/SR.2026.011625

S, 45.4194° W; 925 m above sea level). The specimens were mounted on frames with a slope of 22° from the horizontal. After 2,160 hours of exposure, an 8.3% reduction in tensile strength was observed, under a total accumulated solar radiation of 1,135.04 MJ/m², including an estimated UV irradiance of 85.13 MJ/m².

Aparicio-Ardila et al. (2021), by exposing nonwoven polypropylene geotextiles (417 g/m²) with an initial tensile strength of 21.00 (±2.11) kN/m on frames inclined at 22° from the horizontal under the environmental conditions of São Carlos, São Paulo (Southeastern Brazil; 819 m above sea level; 22°00′19″ S, 47°53′59″ W), observed a 38.8% reduction in tensile strength after the first year and more than 80% after three years. These results were associated with accumulated UV irradiance values of 45.65 MJ/m² and 128.04 MJ/m² for one and three years, respectively.

Carneiro & Lopes (2017) evaluated the chemical stabilization of nonwoven polypropylene geotextiles by incorporating hindered amine light stabilizer (HALS) and carbon black in different proportions before field exposure in Maia, Portugal (41°13′ N, 8°39′ W; 49 m above sea level). The formulations tested were: (i) without additives; (ii) 0.20% HALS; (iii) 0.40% HALS; and (iv) 0.20% HALS + 1.08% carbon black, applied to geotextiles with areal densities ranging from 263 to 284 g/m². The specimens were mounted on racks inclined at 30° from the horizontal. After 12 months of exposure to a total solar radiation of 5,612 MJ/m² and an average temperature of 17.2 °C, the unprotected material exhibited severe degradation and approximately 95% tensile strength loss, being almost destroyed by 18 months. In contrast, stabilized samples retained residual strength after 36 months, under an accumulated solar radiation of 15,086 MJ/m², with the formulation containing 0.20% HALS + 1.08% carbon black preserving more than 60% of the initial tensile properties.

This behavior, observed in both non-stabilized and chemically stabilized materials, was also reported by Carneiro et al. (2018) in field tests conducted under a highly severe coastal environment. Nonwoven polypropylene geotextiles (280 g/m²) were evaluated under the following conditions: without additives (100% PP); with 0.20% HALS (99.80% PP); and with 0.20% HALS + 1.08% carbon black (98.72% PP). The specimens were exposed to natural weathering (on frames inclined at 30° from the horizontal - 38°25′ N, 28°24′ W, 24 m above sea level), seawater immersion (38°31′ N, 28°37′ W), and tidal action (38°32′ N, 28°37′ W). Natural weathering was the most deleterious factor. After 12 months, the non-stabilized geotextile showed complete degradation, whereas the stabilized samples retained tensile strength after 36 months, with reductions of 80.31% (HALS) and 40.34% (HALS + carbon black), consistent with the results reported by Carneiro & Lopes (2017) under less severe exposure conditions.

An additional aspect of degradation phenomena was reported by Carneiro et al. (2019), who compared laboratory and field tests on nonwoven polypropylene geotextiles stabilized with 0.4% HALS, with an initial tensile strength of 27.6 (±0.8) kN/m. In the laboratory, specimens were exposed to cumulative UV radiation of 35 MJ/m² (21 days), 69 MJ/m² (42 days), and 138 MJ/m² (84 days) at 60°C. In the field, geotextiles were subjected to natural weathering in Maia, Portugal (41°13′ N, 8°39′ W; 49 m above sea level) on frames inclined at 30°, for periods of 6, 12, and 24 months. Environmental conditions of temperature and UV levels were as follows: (i) 14°C and 164 MJ/m²; (ii) 17.8°C and 421 MJ/m²; (iii) 17.6°C and 711 MJ/m², corresponding to 6, 12, and 24 months, respectively. Despite the higher UV levels in the field, laboratory tests caused greater reductions in tensile strength; for example, after 42 days of exposure (69 MJ/m²), the residual strength was 53.6%, compared with 72.1% after 24 months of natural weathering. The authors attributed this difference to the higher degradation temperature in the laboratory and to the protective effect of dirt accumulated on field-exposed specimens, which reduced direct UV exposure.

In this context, two aspects deserve attention. The first concerns the limited study of woven geotextiles in field tests, as reported by Guimarães et al. (2017), who analyzed the material over a short period. Comparing the response of woven geotextiles in longer-term tests alongside nonwoven ones may support a more informed selection and application of textile materials, since, in some cases, woven elements exhibit higher tensile strength for the same thickness as nonwoven counterparts. This aspect is particularly relevant in coastal protection works, which are subjected to severe environmental conditions.

The second aspect concerns the methodologies applied in field exposure tests. Although the authors adopted a similar approach (Aparicio-Ardila et al., 2021; Guimarães et al., 2017) — conducting tests on inert racks in accordance with ISO 877-2 (ISO, 2009) — the inclination varied according to latitude and was set at 30° (Carneiro et al., 2018, 2019; Carneiro & Lopes, 2017). Furthermore, there is considerable variation among the technical standards governing these tests. ASTM D1435 (2020), for instance, recommends the use of racks inclined at different angles, made of inert, perforated materials to ensure adequate ventilation. In contrast, ASTM D5970 (ASTM, 2021) specifies the use of racks with a fixed 45° inclination relative to the horizontal, constructed from varnished marine-grade plywood.

Given the need to investigate the performance of geosynthetics in aggressive environments, this study aims to assess the durability of woven polypropylene geotextiles exposed to severe environmental conditions in a coastal zone, through long-term field tests. The materials will be installed on surfaces with distinct characteristics, as well as on similar bases with controlled variations in color and inclination. The research seeks to understand how these factors influence degradation mechanisms over time. The proposed approach aims to support the technical foundation for the more efficient use of these materials in coastal environments.

2. Materials and methods

2.1 Materials properties

White woven polypropylene geotextile was used as the base material for this investigation. The geotextile properties are summarized in Table 1.

The samples were cut to dimensions of 35 cm x 60 cm, with the largest dimension in the transverse direction, and exposed in the field detailed in the following sections.

2.2 Exposure conditions and degradation

The samples were subjected to environmental exposure in five distinct surface configurations, designed to meet the recommendations of ASTM D5970 (ASTM, 2021) and ASTM D1435 (ASTM, 2020a) standards while replicating representative field application scenarios. Four of these configurations were mounted on marine-grade plywood tables, with variations in both the inclination and the surface color to investigate the impact of these factors on weathering. The fifth configuration consisted of a polyvinyl chloride (PVC) box filled with sand, which allowed for direct contact between the geotextile and the granular substrate, thus simulating typical conditions encountered in coastal engineering applications. The use of PVC was justified by its operational simplicity and its suitability for the required study dimensions.

The marine-grade plywood tables, measuring 220 cm x 80 cm, were utilized in strict adherence to standard guidelines. Specifically, ASTM D5970 (ASTM, 2021) and ASTM D1435 (ASTM, 2020a) mandate, respectively, the fixation of test coupons onto a wooden structure and the use of inert material during the exposure period. The sand box, with internal dimensions of 40 cm x 75 cm, represented a specific experimental condition, simulating the direct contact between the geotextile and the sand substrate.

Three inclination angles relative to the horizontal were adopted in the configurations: 0°, 6°, and 45°. The 0° angle (horizontal) was applied exclusively to the sand box, simulating direct contact with the foundation soil. The 6° angle, corresponding to the latitude of the exposure site, allowed comparisons with field tests conducted in different regions, as recommended by ASTM D1435 (ASTM, 2020a). Finally, the 45° inclination followed the guidelines of ASTM D5970 (ASTM, 2021), which establishes that the specimens should be fixed at this angle for weathering tests.

To assess the effect of thermal radiation absorption and reflection, surface color was included as an additional factor. The tabletops of the wooden tables were painted black and white, defining the five test conditions as follows: (i) a pair of black tables inclined at 6° and 45°; (ii) a pair of white tables at the same inclinations; and (iii) the sandbox positioned horizontally (0°). The group names and exposure durations are summarized in Table 2.

The samples were secured to the tables with clamps and anchored to the sandboxes using a polyamide mesh placed above the assembly. Upon completion of this step, the apparatus was transported to the test site and positioned aligned with the Equator line, as illustrated in Figure 1.

The total duration of the test and the sampling intervals were planned in accordance with the guidelines of ASTM

Table 1. Woven geotextile parameters.

Properties	Test method	Reference value
Mass per unit area	ABNT NBR ISO 9864 (ABNT, 2013a)	269 g/m^2
Thickness		1.11 mm
Machine direction tensile strength	ABNT NBR ISO 10319 (ABNT, 2013b)	50 kN/m
Cross machine direction tensile strength		50 kN/m
Tear resistance	ASTM D4533 (ASTM, 2020b)	0.50 kN/m
Puncture resistance	ABNT NBR 13359 (ABNT, 1995)	5 kN
Permittivity	ASTM D4491 (ASTM, 2017)	0.02 l/s
Apparent opening size (95%)	AFNOR G 38017 (AFNOR, 1989)	100 mm

Table 2. Field exposure groups.

Identification	Surface	Inclination	Exposure Time (days)
G0	-	-	0
GB6	Black table	6°	41, 83, 175, 492
GB45	Black table	45°	41, 83, 175, 492
GW6	White table	6°	41, 83, 175, 492
GW45	White table	45°	41, 83, 175, 492
GS	Sandbox	0°	41, 83, 175, 492

Figure 1. Field test in operation with tables inclined at 45° and sandboxes inclined at 0°.

D5970 (2021), establishing a total exposure period of 540 days. Sample collections were conducted at 41, 83, 175, and 492 days of exposure. The progression of these intervals was determined by the successive doubling of the period following the first collection, as recommended by the standard, with minor adjustments made for operational reasons. This experimental design allowed for the assessment of material degradation both before (175 days) and after (492 days) the 12-month mark. The adoption of this extended sampling strategy was based on previous studies, such as Carneiro et al. (2018) who reported significant degradation of nonwoven geotextiles in coastal environments around 360 days of exposure.

2.3 Geographic and climate characteristics of field exposure

The material was exposed in a coastal environment in the city of Natal, capital of Rio Grande do Norte, located at 30 m altitude, with 5º 47’ 42’’ south latitude and 35º 12’ 34’’ west longitude, at the Department of Oceanography and Limnology of the Federal University of Rio Grande do Norte (DOL/UFRN), located 80 meters from the Atlantic Ocean, with a start date of January 22, 2022, and an end date of May 29, 2023.

According to Köppen’s classification (Peel et al., 2007), the region has a tropical savanna climate (Aw), with high temperatures and humidity most of the year, a distinct dry season, and annual rainfall above 1,200 mm, often acidic due to the influence of the Intertropical Convergence according to Zone Lopes et al. (2015).

To characterize the environmental seasonality throughout the 492-day study period, variables including global radiation, temperature, precipitation, and relative humidity were analyzed. These data were sourced from the meteorological database of the National Institute of Meteorology (INMET, 2025), obtained from both the automatic NATAL station (A304) and the conventional NATAL station (82590), located 5,500 m away from the testing site.

The data from the conventional station were primarily used to complement the information missing from the automatic station bulletins and the radiation, in this case, was estimated through the hours of daily sunshine using the equation Ångström-Prescott (Medeiros et al., 2017) (Equation 1).

$$H/H_0 = a + b\left(\frac{n}{N}\right) \tag{1}$$

where H is the estimated global solar radiation, H_0 is the extraterrestrial radiation, a and b are local adjustment coefficients, n is the actual daily sunshine duration in hours, and N is the maximum possible sunshine duration. The calculation of extraterrestrial radiation was performed using Equation 2.

$$H_0 = \frac{86.400\, I_{sc}}{\pi} E_0 \left[\omega_s \sin(\phi)\sin(\delta) + \cos(\phi)cos(\delta)\sin(\omega_s)\right] \tag{2}$$

The parameters I_{sc}, E_0, ω_s, ϕ and δ, represent the solar constant (assumed to be 1367 W/m^2), the eccentricity correction factor for the day of the year, the sunset hour angle, the latitude (adopted as -0.10145 radians), and the solar declination, respectively.

It is also noteworthy that the local adjustment coefficients used were a = 0,29 e b = 0,41, according to the study by Medeiros et al. (2017) conducted in the city of Natal, RN. The other variables involved were obtained based on latitude and the day of the year, counted from 1 to 365, since 2022 was not a leap year.

The main information on temperature, global radiation, precipitation, and relative humidity for 492 days is summarized in Figure 2.

The wind regime in the study area is characterized by a strong Southeast (SE) quadrant predominance, as indicated by the modal azimuth of 141°. This persistent directionality is consistent with the influence of Trade Winds. The mean wind speed of 10.69 km/h reflects a steady flow, with observed extremes ranging from a minimum of 6 km/h to a maximum of 17 km/h.

Directional variations are minimal and isolated, with the majority of occurrences concentrated between East-Southeast (ESE, ~134°) and South-Southeast (SSE, ~141°). Rare and punctual deviations were recorded at the angular extremes of Northeast (NE) and South-Southwest (SSW), which do not reflect the dominant eolian regime.

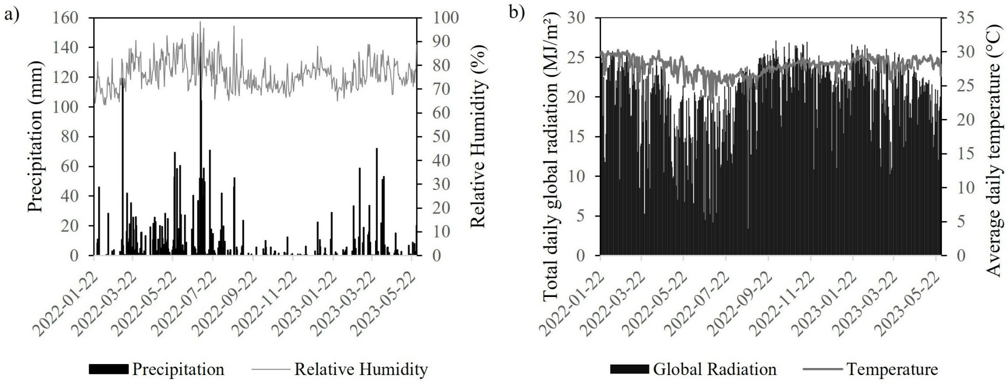

Figure 2. Environmental characterization of the exposure period. a) Precipitation and relative humidity. b) Global radiation and average daily temperature.

Given the low frequency and isolated nature of the observed variations in the local wind regime, the subsequent discussion will primarily focus on the variables of radiation, temperature, precipitation, and humidity, which exert a greater influence on the subject under investigation.

The first exposure period of 41 days started on 01/22/2022 and lasted until 03/04/2022. Its main characteristic was the higher temperatures, with an average of 29.37°C, explained by the occurrence of the summer solstice in the Southern Hemisphere.

The second period, comprising 83 days of exposure, lasting until 04/15/2022, shows a notable reduction in average temperature when compared to the first 41 days, justified by the presence of the autumnal equinox in the southern hemisphere, starting on 03/21/2022. In this season, the hours of day and night are equal, reducing the time of sunlight compared to the summer solstice. The maximum daily global radiation of the second period is the same as the first, having occurred in February.

The 175-day exposure, ending on 07/16/2022, showed a reduction in the average temperature of almost 2°C compared to period 1, alone. This is because in addition to the autumn equinox, there was the inclusion of part of the winter solstice, which began on 06/21/2022.

The final interval, lasting 492 days and ending on 05/29/2023, exposed the geotextiles to the full range of environmental seasonality across all four seasons. It is worth noting that between periods 3 and 4, both temperature and solar radiation increased, while relative humidity, as well as the frequency and duration of precipitation, showed a noticeable decline. During this interval, the spring and autumn equinoxes, along with the summer solstice, were predominant, with maximum solar radiation reaching 27.1 MJ/m^2 on 10/02/2022.

It is noteworthy that the cumulative global solar radiation recorded during the exposure periods was 935.5 MJ/m^2 (41 days), 1760.5 MJ/m^2 (83 days), 3242.1 MJ/m^2 (175 days), and 10076.5 MJ/m^2 (492 days). These values can be estimated in terms of ultraviolet (UV) radiation using the percentage range defined by Greenwood et al. (2012), who indicate that UV radiation typically represents between 5% and 10% of the global solar radiation, depending on location-specific factors such as altitude and latitude. In this case, a value of 7.5% was adopted due to the site's proximity to the equator. Accordingly, the estimated cumulative UV radiation for the respective intervals was 70.16 MJ/m^2, 132.04 MJ/m^2, 243.16 MJ/m^2, and 755.74 MJ/m^2.

The assessment of geotextile deterioration was conducted mechanically through narrow strip tensile tests, performed in accordance with ASTM D 5035 (ASTM, 2008). The tests were carried out at the Geotechnical and Geosynthetics Laboratory of the Federal University of São Carlos (LabGeo/UFSCar).

To validate the results obtained from the tensile strength tests, statistical analyses employing confidence intervals were prioritized. Given the small sample size ($n < 30$), the normality of the distribution was assessed using the Shapiro-Wilk test, which considers two possible hypotheses: the null hypothesis (H0) that the strengths are normally distributed, and the alternative hypothesis (H1) that the strengths are not normally distributed.

In the event of H0, the calculation proceeded using the student's t-test methodology; in the event of H1, a resampling procedure was adopted. The entire statistical analysis was performed using R Studio software.

3. Analysis and results

The in-field degradation of the geotextiles was primarily quantified by the reduction in mechanical strength, assessed via the wide-width strip tensile test. Nevertheless, visual inspections were conducted periodically to identify the occurrence of fiber ruptures, pigmentation, and the accumulation of debris, all of which indicate damage promoted by the exposure conditions. Only the samples subjected to 492 days of natural weathering exhibited perceptible visual changes, including fiber splitting and soiling accumulation, as illustrated in Figure 3 compared to the reference material.

As illustrated in Figure 3, the exposed geotextile samples exhibit microcracks within the fibers and noticeable impregnation of biological material (biofouling). This finding is consistent with the local climatic regime, which favors the development of microorganisms and biofilms (e.g., algae and sludge) on the material's surface. However, the identification of isolated microcracks is not adopted as an exclusive criterion for degradation, given that the filaments already presented intrinsic structural variations in the intact (virgin) condition. A detailed assessment of the mechanical resistance and complementary properties of the geotextiles is presented in the subsequent sections.

3.1 Influence of surface inclination

The results of the tensile tests of the samples on a white support inclined at latitude and 45° are shown in Figure 4. In terms of tensile strength, the values were similar between the two slopes for all periods studied, with the greatest difference observed at time 2 (83 days). Condition GW6 maintained the resistance at 43.38 kN/m, while GW45 presented a value of 39.99 kN/m, with a difference of 3.99 kN/m (7.81%) between the conditions. This divergence is not significant since at some points the samples share the same confidence interval, as further discussed in Section 3.3

In the other periods, this difference did not exceed 3%, with alternating conditions observed in the minimum tensile strength values. For instance, in period 1 (41 days), condition GW6 presented a mean value of 47.58 kN/m, while GW45 showed 48.11 kN/m. In period 3 (175 days), the GW6 group resulted in 40.23 kN/m, whereas GW45 recorded a tensile strength value of 39.21 kN/m.

Of note is that, at the end of the exposure period (492 days), both conditions experienced a loss of between 32% and 34% of their original properties, with values of 32.77 kN/m for the latitude inclination and 33.70 kN/m for the 45° inclination.

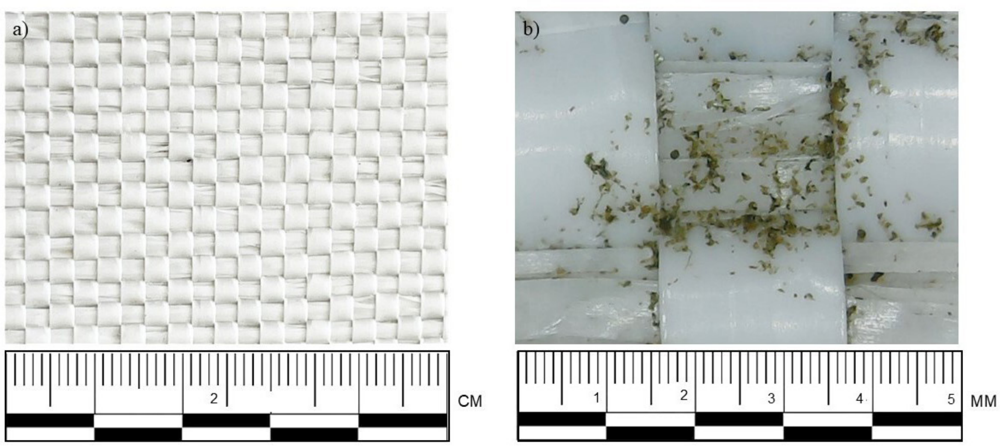

Figure 3. a) Intact woven geotextile. b) Geotextile after 492 days of exposure (degraded condition).

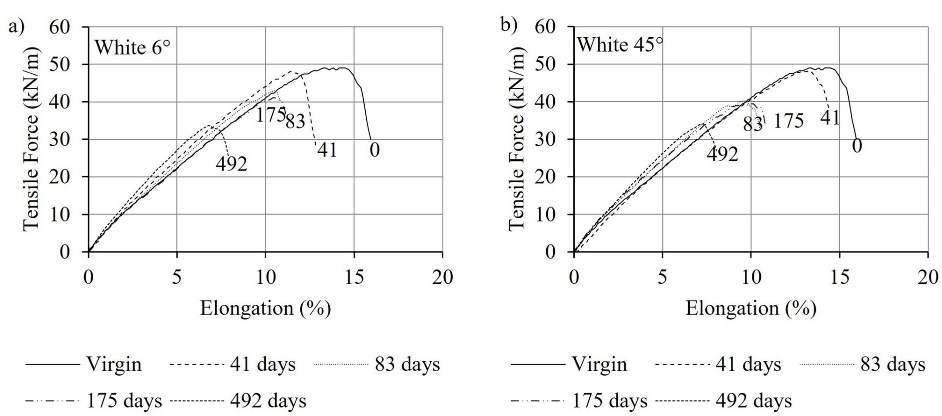

Figure 4. Results of tensile strength tests with support at different inclinations in white. a) GW6 – inclination at latitude. b) GW45 – inclination at 45°.

3.2 Effect of type of surface

In Figure 5, the GW6 and GB6 groups were expressed in the results of the narrow strip tensile strength test for all periods.

At 41 days, the values were similar, with a slight reduction in tensile strength observed in sample GB6, measuring 46.45 kN/m compared to 47.58 kN/m for group GW6. Conversely, in the subsequent periods, surface color exerted a greater influence, with lower strength values recorded for the black condition. The same trend was observed on surfaces inclined at 45°, where the black color led to more pronounced deterioration, except at the 83-day exposure, when GW45 exhibited a tensile strength 0.48 kN/m lower than GB45 (Figure 6).

The GS group, represented by the sand surface inclined at 0°, is illustrated in Figure 7. Under this condition, degradation progressed at rates of 3%, 17%, 25%, and 33%. A 14% increase between periods 1 and 2 can be attributed to environmental factors, as the deterioration agents acted synergistically: precipitation and relative humidity increased compared to period 1, while high temperatures and global radiation were maintained with only a slight decrease.

The rate of degradation for the material in contact with the sand substrate remained comparable to that observed under the other exposure conditions on the test benches. This finding suggests substrate inertness, indicating that the sand and the marine plywood behaved in a similarly neutral manner with respect to the geotextile. Overall, the material's behavior, as illustrated in Figures 4 and 6, was similar to that of groups GW6 and GW45, exhibiting slightly lower degradation rates compared to the GB group conditions. However, this general trend was exceptionally reversed in Period 3, when this specific condition (sand) recorded the highest degradation index, reaching 37.17 kN/m.

3.3 Confidence interval analysis

The Shapiro-Wilk tests demonstrated that all samples followed a normal distribution, with the null hypothesis

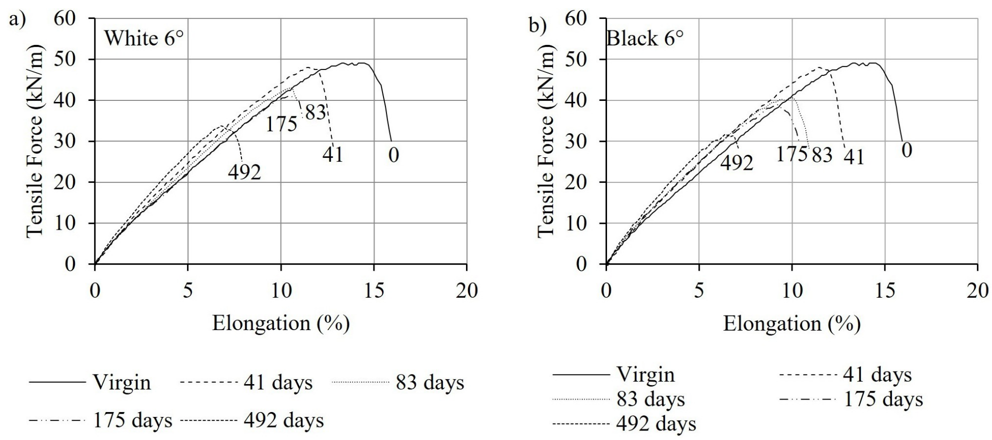

Figure 5. Results of tensile strength tests with supports on different inclined surfaces in latitude. a) GW6 – white color. b) GB6 – black color.

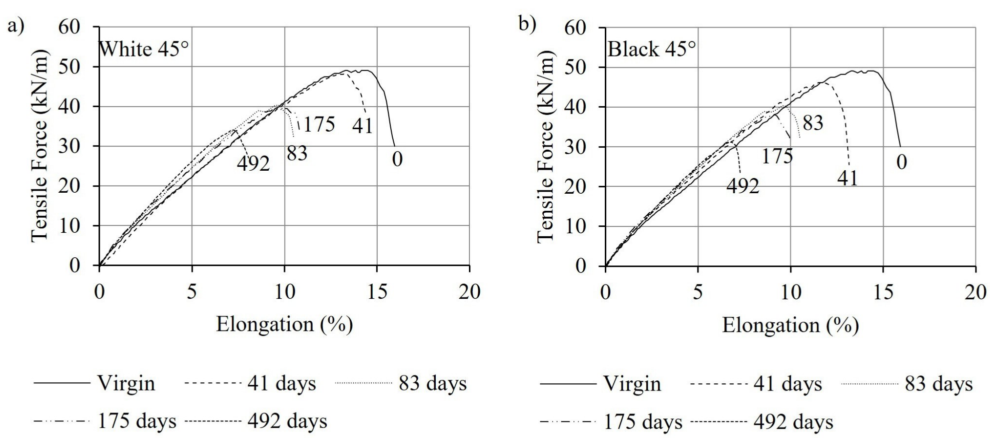

Figure 6. Results of tensile strength tests with supports on different surfaces inclined at 45°. a) GW45 – white color. b) GB45 – black color.

H0 accepted. The 95% confidence interval calculated is presented in Figure 7.

The combined analysis of the first period reveals a slight tendency for more pronounced degradation in samples exposed on black surfaces, especially when inclined at 45°, as demonstrated by the group's position to the left of the confidence interval of the intact condition. This indicates that mechanical properties of the geotextile were already altered within the first 41 days.

At 83 days, all groups were positioned to the left of the confidence interval of the intact condition, proving the degradation of the material. During this period, there was no preponderance of the slope or the type of surface in the degradation, with an overall average of 41.18 kN/m of tensile strength. The only exception occurred in group GW6, which differs from the others and does not maintain intersection with the data of GB6 or GB45. This may be associated with sample variability, since the same conditions were maintained in the tests for all groups.

The same phenomenon was observed at 175 days, with a slight deviation of GW6 compared to the other groups. However, it is important to note that the confidence intervals overlapped among the other conditions, except for the sand, which caused greater material wear during this period.

At the end of the exposure, after 492 days, there was a predominance of deterioration on the black surfaces, mainly the one inclined at 45°, which presented an average tensile strength value equal to 30.59 kN/m, with a reduction of almost 40% in the initial value of the intact condition.

A percentage close to 40% was also reported by (Aparicio-Ardila et al., 2021) at the end of the first year of natural weathering exposure of a nonwoven polypropylene geotextile, with the support inclined at the latitude angle, in the city of São Carlos (20°00′11″S; 47°53′57″W), in southeastern Brazil, under less aggressive environmental conditions.

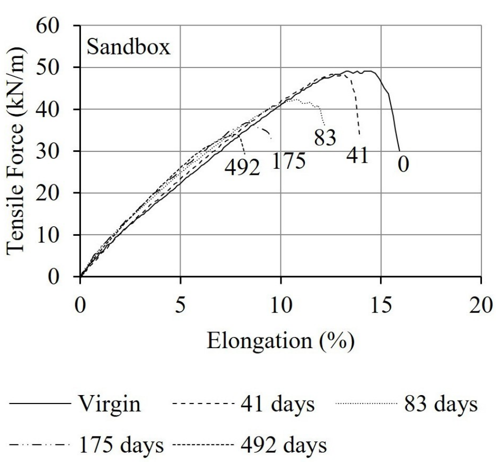

Figure 7. Tensile strength test results for samples overlying sand at 0° inclination.

The analysis of Figure 8 may indicate a greater need to consider the surfaces used in field exposure tests. This is because, under the same environmental conditions, mechanical responses may not coincide within the same confidence interval for a given inclination, as observed at 492 days between groups GB45 and GW45.

3.4 Additional mechanical parameters

The data regarding maximum tensile strength, elongation at break, and degradation rates were compiled and are presented in Figure 9.

According to Figure 9, the maximum tensile strength exhibited a progressive reduction over the exposure period, reaching an approximate loss of 40% relative to the material's original properties after around 500 days of exposure. Similarly, the elongation at maximum load decreased from approximately 15% for the unexposed sample to about 7% after 492 days, representing a reduction of roughly 50%. Although the results for intermediate exposure times show minor variations, both tensile strength and elongation consistently demonstrate a decreasing trend, indicating the influence of environmental conditions on the degradation of the geotextile's mechanical properties. Part of these variations can also be attributed to inherent material heterogeneities, as previously discussed in the confidence interval analyses.

The combined evaluation of tensile strength and elongation was conducted by calculating the geotextile stiffness, defined as the ratio of maximum stress to corresponding strain. Figure 10 shows the evolution of stiffness over the exposure period.

During the first 200 days, stiffness fluctuated mainly between 300 and 400 kN/m. After approximately 500 days of exposure, stiffness consistently increased, approaching 450 kN/m across all conditions. This trend indicates material hardening, likely due to polymer degradation and the resulting reduction in the geotextile's deformation capacity.

Geotextile stiffening due to prolonged exposure to environmental factors, such as ultraviolet radiation, temperature fluctuations, and salinity, can significantly compromise the performance and durability of protective systems in which it is used. Increased stiffness reduces the material's deformation capacity, affecting soil–geosynthetic interaction in structures subjected to differential settlements, movements, or hydraulic impacts. Reduced ductility limits stress redistribution, promoting localized stress concentrations and increasing the risk of fatigue or premature failure. From a hydraulic perspective, decreased flexibility can impair the geotextile's filtration behavior by altering its contact with the soil surface and promoting preferential flow paths, thus increasing the risk of internal erosion. In coastal protection systems or slope coverings, these effects may lead to the loss of fine particle confinement, surface instability, and reduced service life of the structure.

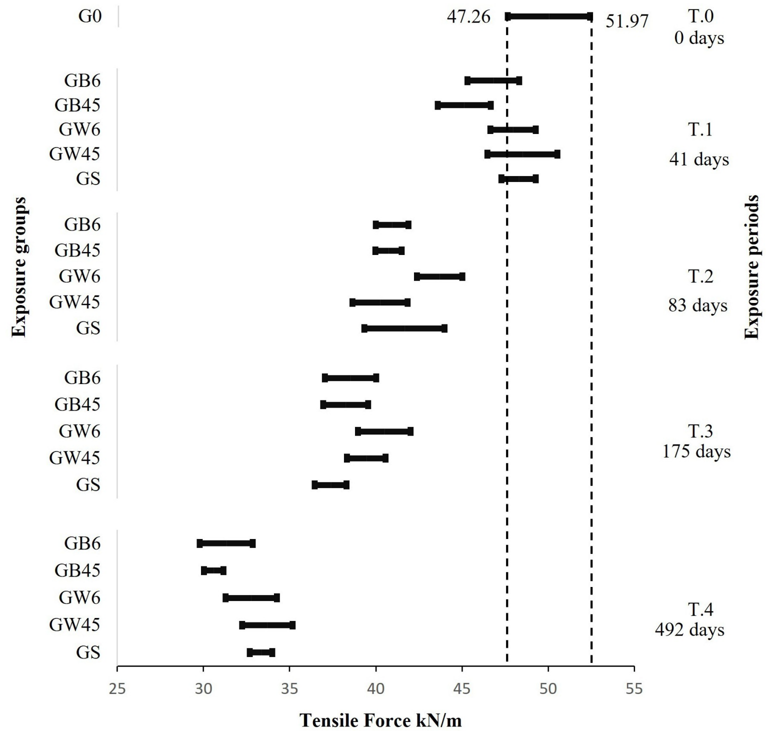

Figure 8. Confidence intervals for all analysis periods.

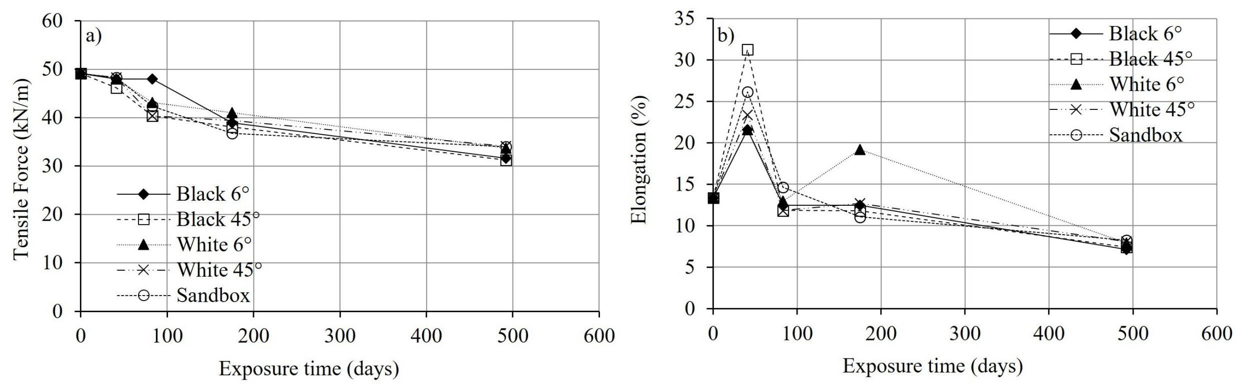

Figure 9. Wide-width tensile test results according to exposure time: a) Maximum tensile strength; b) Elongation at break.

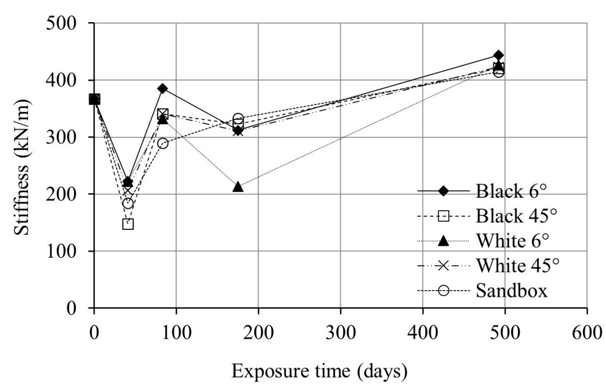

Figure 10. Stiffness as a function of exposure time.

4. Conclusion

This study evaluated the durability of a woven polypropylene geotextile subjected to natural weathering in a coastal environment for 492 days. Among the main variables, the influence of the surface on the degradation observed through narrow strip tensile strength tests was investigated. Based on this, the main conclusions can be summarized as follows:

- The color of the surface may be a point of attention when conducting the test, especially in regions of high temperatures and radiation levels due to energy absorption, which may delay heat dissipation between the exposure surface and the environment and keep the samples in deleterious conditions for a long time;
- In general, the surface inclination did not significantly influence the divergence of results in the tensile strength tests.
- Environmental conditions have a strong influence on the degradation process, especially when associated with high temperatures, radiation levels, and rainfall, promoting polymer oxidation.
- At the end of the 492 days, the samples lost approximately 34.8% of their initial properties, with emphasis on period 2, in which the materials already presented a variation of 17% in this parameter.
- The group that degraded the most at the end of the period was GB45 with an average of 30.59 kN/m. This difference was also seen at 41 days due to environmental conditions.

Acknowledgements

The authors would like to thank the Coordination for the Improvement of Higher Education Personnel (CAPES) for funding the equipment, DOL/UFRN for providing the facilities for the study, and LabGeo/UFSCar for conducting the laboratory tests.

Declaration of interest

The authors have no conflicts of interest to declare. All co-authors have observed and affirmed the contents of the paper and there is no financial interest to report.

Authors' contributions

Rayanne Karlla Santos da Silva: conceptualization, data curation, investigation, visualization, writing – original draft. Lucas Araújo dos Santos: methodology, formal analysis, validation, writing – original draft. Fagner Alexandre Nunes de França: funding acquisition, investigation, methodology, project administration, resources, supervision, validation, writing – review & editing. Matheus Cardoso dos Santos: methodology, writing – review & editing. Fernando Henrique Martins Portelinha: supervision, validation, writing – review & editing.

Data availability

The datasets generated analyzed in the course of the current study are available from the corresponding author upon request.

Declaration of use of generative artificial intelligence

This work was prepared with the assistance of generative artificial intelligence (ChatGPT) with the aim of translation. The entire process of using this tool was supervised, reviewed and when necessary edited by the authors. The authors assume full responsibility for the content of the publication that involved the aid of ChatGPT.

List of symbols and abbreviations

a	Linear coefficient of the Angström-Prescott equation
b	Angular coefficient of the Angström-Prescott equation
n	Actual daily sunshine duration
E_o	Eccentricity correction factor for the day of the year
HALS	Hindered Amine Light Stabilizer
H	Daily estimated global solar radiation
H_o	Daily Extraterrestrial radiation
I_{sc}	Solar constant
N	Daily maximum sunshine duration
UV	Ultraviolet
δ	Solar declination
ϕ	Latitude
ω_s	Sunset hour angle

References

ABNT NBR 13359. (1995). *Geotextiles - Determination of static puncture resistance - CBR type wire test*. ABNT - Associação Brasileira de Normas Técnicas, Rio de Janeiro.

ABNT NBR ISO 10319. (2013a). *Geosynthetics — Wide-width tensile test*. ABNT - Associação Brasileira de Normas Técnicas, Rio de Janeiro.

ABNT NBR ISO 9864. (2013b). *Geosynthetics — Test method for the determination of mass per unit area of geotextiles and geotextile-related products*. ABNT - Associação Brasileira de Normas Técnicas, Rio de Janeiro.

AFNOR G 38017. (1989). *Geotextiles — Test methods for hydraulic properties*. AFNOR - French Association for Standardization, Paris.

Aparicio-Ardila, M.A., Pedroso, G.O.M., Kobelnik, M., Valentin, C.A., da Luz, M.P., & Lins da Silva, J. (2021). Evaluating the degradation of a nonwoven polypropylene geotextile exposed to natural weathering for 3 years. *International Journal of Geosynthetics and Ground Engineering*, 7(3), 69. https://doi.org/10.1007/s40891-021-00314-6.

ASTM D1435-20. (2020a). *Standard Practice for Outdoor Weathering of Plastics*. ASTM International, West Conshohocken, PA. https://doi.org/10.1520/D1435-20.

ASTM D4533-20. (2020b). *Standard Test Method for Trapezoid Tearing Strength of Geotextiles*. ASTM International, West Conshohocken, PA. https://doi.org/10.1520/D4533-20.

ASTM D4491-17. (2017). *Standard Test Methods for Water Permeability of Geotextiles by Permittivity*. ASTM International, West Conshohocken, PA. https://doi.org/10.1520/D4491-17.

ASTM D5035-08. (2008). *Standard Test Method for Breaking Force and Elongation of Textile Fabrics (Strip Method)*. ASTM International, West Conshohocken, PA. https://doi.org/10.1520/D5035-08.

ASTM D5970-21. (2021). *Standard Practice for Preparation of Soil and Control of Moisture Content for Fabrication of Geotextile Test Specimens*. ASTM International, West Conshohocken, PA. https://doi.org/10.1520/D5970-21.

Carneiro, J.R., & Lopes, M.L. (2017). Natural weathering of polypropylene geotextiles treated with different chemical stabilisers. *Geosynthetics International*, 24(6), 544-553. https://doi.org/10.1680/jgein.17.00020.

Carneiro, J.R., Almeida, P.J., & Lopes, M.L. (2019). Evaluation of the resistance of a polypropylene geotextile against ultraviolet radiation. *Microscopy and Microanalysis*, 25(6), 1512-1521. https://doi.org/10.1017/S1431927618000430.

Carneiro, J.R., Morais, M., & Lopes, M.L. (2018). Degradation of polypropylene geotextiles with different chemical stabilisations in marine environments. *Construction & Building Materials*, 165, 877-886. https://doi.org/10.1016/j.conbuildmat.2018.01.067.

Elias, T., Geetha, T., & Shirlal, K.G. (2022). Effect of armour unit layers and placement mode in the determination of stability of geotextile sand container (GSC) breakwaters. *Geotextiles and Geomembranes*, 50(3), 444-454. https://doi.org/10.1016/j.geotexmem.2022.01.003.

Greenwood, J.H., Schroeder, H.F., & Voskamp, W. (2012). *Durability of geosynthetics* (CUR Report, No. 242). CUR.

Guimarães, M.G.A., de Mattos Vidal, D., de Carvalho Urashima, D., & Castro, C.A.C. (2017). Degradation of polypropylene woven geotextile: tensile creep and weathering. *Geosynthetics International*, 24(2), 213-223. https://doi.org/10.1680/jgein.16.00029.

Hsieh, C.W., Wang, J.B., & Chiu, Y.F. (2006). Weathering properties of geotextiles in ocean environments. *Geosynthetics International*, 13(5), 210-217. https://doi.org/10.1680/gein.2006.13.5.210.

Instituto Nacional de Meteorologia do Brasil – INMET. (2025). *Banco de dados meteorológicos para ensino e pesquisa*. Retrieved in July 31, 2025, from https://bdmep.inmet.gov.br/. (in Portuguese).

ISO 877-2. (2009). *Plastics – Methods of exposure to solar radiation – Part 2: Direct weathering and exposure behind window glass*. International Organization for Standardization, Geneva, Switzerland.

Koerner, R.M., Lord Junior, A.E., & Hsuan, Y.H. (1992). Arrhenius modeling to predict geosynthetic degradation. *Geotextiles and Geomembranes*, 11(2), 151-183. https://doi.org/10.1016/0266-1144(92)90042-9.

Li, Y., You, Z.J., Ma, Y., & Ren, B. (2023). Quantitative assessment of the shoreline protection performance of geotextile sandbags at an in-situ coastal experimental station. *Geotextiles and Geomembranes*, 51(3), 371-380. https://doi.org/10.1016/j.geotexmem.2023.01.001.

Lopes, D.P., Alves, A.E.L., Souza, M.R., & Silva, F.M. (2015). Comportamento estatístico do grau de acidez das chuvas na cidade de Natal/RN pela distribuição Gaussiana (Statistical behavior of rainwater acidity in Natal/RN using the Gaussian distribution). *HOLOS*, 6, 83-89. https://doi.org/10.15628/holos.2014.2175.

Medeiros, F.J., Silva, C.M.S., & Bezerra, B.G. (2017). Calibration of Ångström–Prescott equation to estimate daily solar radiation on Rio Grande do Norte State, Brazil. *Revista Brasileira de Meteorologia*, 32(3), 409-461. https://doi.org/10.1590/0102-77863230008.

Paula, A.M., & Pinho-Lopes, M. (2021). Constitutive modelling of short-term tensile response of geotextile subjected to mechanical and abrasion damages. *International Journal of Geosynthetics and Ground Engineering*, 7(3), 1-11. https://doi.org/10.1007/s40891-021-00313-7.

Peel, M.C., Finlayson, B.L., & McMahon, T.A. (2007). Updated world map of the Köppen-Geiger climate classification. *Hydrology and Earth System Sciences*, 11(5), 1633-1644. https://doi.org/10.5194/hess-11-1633-2007.

Rajabian, A., Viswanadham, B.V.S., Ghiassian, H., & Salehzadeh, H. (2012). Centrifuge model studies on anchored geosynthetic slopes for coastal shore protection. *Geotextiles and Geomembranes*, 34, 144-157. https://doi.org/10.1016/j.geotexmem.2012.06.001.